

	001
	002
	003
	004
	005
Distinct contributions of anterior and posterior orbitofrontal cortex to adaptive decision-making	006
	007
	008
	009
	010
Qingfang Liu <sup>1</sup> , Daria Porter <sup>2</sup> , Hadeel Damra <sup>2</sup> , Yao Zhao <sup>3</sup> ,	011
Joel L. Voss <sup>4</sup> , Geoffrey Schoenbaum <sup>1</sup> , Thorsten Kahnt <sup>1*</sup>	012
<sup>1</sup> National Institute on Drug Abuse Intramural Research Program,	013
Baltimore, 21224, MD, USA.	014
<sup>2</sup> Feinberg School of Medicine, Northwestern University, Chicago, 60611,	015
IL, USA.	016
<sup>3</sup> Department of Psychology, University of Pennsylvania, Philadelphia,	017
19104, PA, USA.	018
<sup>4</sup> Department of Neurology, The University of Chicago, Chicago, 60611,	019
IL, USA.	020
*Corresponding author(s). E-mail(s): <a href="mailto:thorsten.kahnt@nih.gov">thorsten.kahnt@nih.gov</a> ;	021
	022
	023
	024
	025
	026
	027
<b>Abstract</b>	028
The lateral orbitofrontal cortex (OFC) is critical for flexibly adjusting choices	029
when outcome values change. This requires representations of stimulus-outcome	030
associations and inferring the current value of outcomes, but whether and how	031
different parts of OFC contribute to these functions has remained unclear. Here	032
we used transcranial magnetic stimulation (TMS) to disrupt activity in func-	033
tional networks centered on the anterior (aOFC) and posterior (pOFC) lateral	034
OFC. Participants (n = 48) received aOFC or pOFC network-targeted TMS	035
either before learning associations between visual stimuli and sweet or savory	036
food odor rewards, or, on the next day, before a meal to selectively devalue one	037
of these rewards. TMS targeting pOFC before the meal disrupted goal-directed	038
behavior, as measured by choices of stimuli predicting non-sated rewards in a	039
probe test, whereas disrupting aOFC before learning stimulus-outcome associ-	040
ations similarly impaired choices in the probe test. These findings demonstrate	041
distinct contributions of different OFC subregions to goal-directed behavior.	042
<b>Keywords:</b> adaptive decision-making, goal-directed behavior, cognitive map,	043
orbitofrontal cortex	044
	045
	046

047 **1 Introduction**

048

049 Humans and animals effortlessly adapt to changing environments by flexibly adjusting  
050 their behavior. This adaptability relies on outcome-guided decision-making, where  
051 individuals can re-evaluate their choices in real time, simulating potential outcomes  
052 based on changes in outcome value (Daw et al, 2005) rather than defaulting to habitual  
053 responses. For example, a restaurant chef might anticipate that a guest could experience  
054 an allergic reaction to certain ingredients and adjust the dish accordingly before  
055 an issue arises. To enable this flexibility, a detailed representation of the environment—  
056 commonly referred to as a cognitive map or model—is essential (Behrens et al, 2018).  
057 A chef with full knowledge of ingredients and associated allergies can efficiently modify  
058 recipes to accommodate allergies without compromising the dish. The orbitofrontal  
059 cortex (OFC) plays a central role in both processes, supporting adaptive behaviors  
060 through the formation of cognitive maps (Costa et al, 2023; Wilson et al, 2014; Wang  
061 and Hayden, 2021) as well as their use to simulate potential outcomes (Howard et al,  
062 2020; Rudebeck and Murray, 2014).

063 The OFC is a heterogeneous region, comprising multiple subregions with varying  
064 anatomical and functional properties along both mediolateral and anterior-posterior  
065 axes (Price, 2007; Wallis, 2012; Kahnt et al, 2012; Izquierdo, 2017; Wang et al, 2022;  
066 Heilbronner et al, 2016; Walton et al, 2011; Mackey and Petrides, 2010; Kringlebach  
067 and Rolls, 2004; Neubert et al, 2015). In humans, studies on value-based decision-  
068 making have primarily focused on the functional distinctions between the medial and  
069 lateral OFC (Kringlebach and Rolls, 2004; Wallis, 2012; Kahnt et al, 2012; Walton  
070 et al, 2011; McNamee et al, 2013; Howard et al, 2015; O'Doherty et al, 2001), whereas  
071 the anterior-posterior axis has received comparatively less attention.

072 The current study aims to identify the distinct roles of anterior and posterior  
073 subregions within the lateral OFC in supporting adaptive behavior in an outcome  
074 devaluation task (Wilson et al, 2014; Howard et al, 2020; Colwill and Rescorla, 1985;  
075 Balleine and Dickinson, 1998; Baxter et al, 2000; Murray et al, 2015; Critchley and  
076 Rolls, 1996; O'doherty et al, 2000; Gottfried et al, 2003; Howard and Kahnt, 2017,  
077 2021; Gallagher et al, 1999; Pickens et al, 2003; Ostlund and Balleine, 2007). Outcome  
078 devaluation assesses responses to predictive cues following the selective devaluation of  
079 their associated outcomes, thereby revealing the capacity to align choices with updated  
080 goals and contexts. In outcome-specific versions of this task, different stimuli are first  
081 associated with different but equally preferred rewards. Next, one of the outcomes is  
082 selectively devalued (for instance by feeding it to satiety), and then choices between  
083 stimuli are assessed in a probe test. While earlier theories emphasized the role of  
084 the OFC in signaling the current value of stimuli to guide response selection (Baxter  
085 et al, 2000), more recent accounts propose two complementary roles: one in using  
086 mental simulations to infer or update the value of outcome-predicting stimuli (Wilson  
087 et al, 2014; Murray et al, 2015; Howard et al, 2020), and another in constructing and  
088 modifying the relevant cognitive map that links stimuli to outcomes during initial  
089 learning (Gardner and Schoenbaum, 2021; Costa et al, 2023). In the current work, we  
090 focus on these latter two mechanisms, proposing a unified framework that integrates  
091 them within the lateral OFC and empirically testing for functional specialization across  
092 subregions.

Previous studies in non-human primates suggest that anterior and posterior regions of the OFC support distinct functions in goal-directed behavior (Murray et al, 2015). Our earlier work further demonstrated that the posterior OFC is critical for retrieving and using stimulus–outcome associations (Howard et al, 2020). Building on these findings, we hypothesized that the anterior and posterior lateral OFC subregions are differentially involved in separate phases of the outcome devaluation task: the anterior OFC during acquisition of stimulus–outcome associations, and the posterior OFC during their retrieval and use in guiding choices. To test this, we applied network-targeted transcranial magnetic stimulation (TMS) with continuous theta burst stimulation (cTBS) either before intial training or before the probe test, in a multi-session within-participant study. This approach allowed us to test the specific roles of anterior and posterior portions of the lateral OFC network for learning associative structures and guiding choices based on current values.

Our findings reveal distinct roles for the anterior and posterior lateral OFC networks in goal-directed behavior. Disruption of the posterior but not anterior lateral OFC network before the probe test impaired adaptive choices, whereas disruption of the anterior but not posterior lateral OFC before initial learning similarly impaired subsequent goal-directed choices in the probe test. Additionally, cTBS targeting either region disrupted value acquisition, but only during the first session. Together, these results suggest that anterior and posterior lateral OFC networks play complementary roles for goal-directed behavior, supporting the acquisition and use of outcome-specific stimulus-reward associations, respectively.

## 2 Results

### 2.1 Experimental design and outcome devaluation task.

This study follows a within-participant, multiple-session design, with 48 healthy human participants completing a two-day experiment, repeated across three separate sessions (spaced at least one week apart; Fig. 1A). Each session involves the delivery of either cTBS on one day and sham TMS on the other, or sham TMS on both days, resulting in three conditions (Day 1-Day 2: cTBS-sham, sham-cTBS, sham-sham, order counterbalanced; Fig. 1D).

On Day 1, participants learned to discriminate pairs of visual stimuli associated with desirable food odors (sweet or savory, equally valued based on pre-task ratings; Fig. 1E) and clean air. They were asked to select the stimulus associated with any odor, meaning they were not required to encode the specific stimulus-outcome identity associations to perform the discrimination task (Fig. 1B, C). On Day 2, participants chose between stimuli based on odor preferences, making choices between stimuli predicting sweet and savory odors, or between stimuli predicting odor and air. A pre-meal free choice task was followed by a meal, then by a post-meal free choice task. Participants received the odors during the Day 1 discrimination task and the Day 2 pre-meal free choice task. No odors were delivered during Day 2 post-meal free choice task. Participants also reported how much they liked each odor before and after the meal.

To explore the potentially distinct functional roles of OFC subregions in this task, TMS was administered at two different time points—either before the discrimination

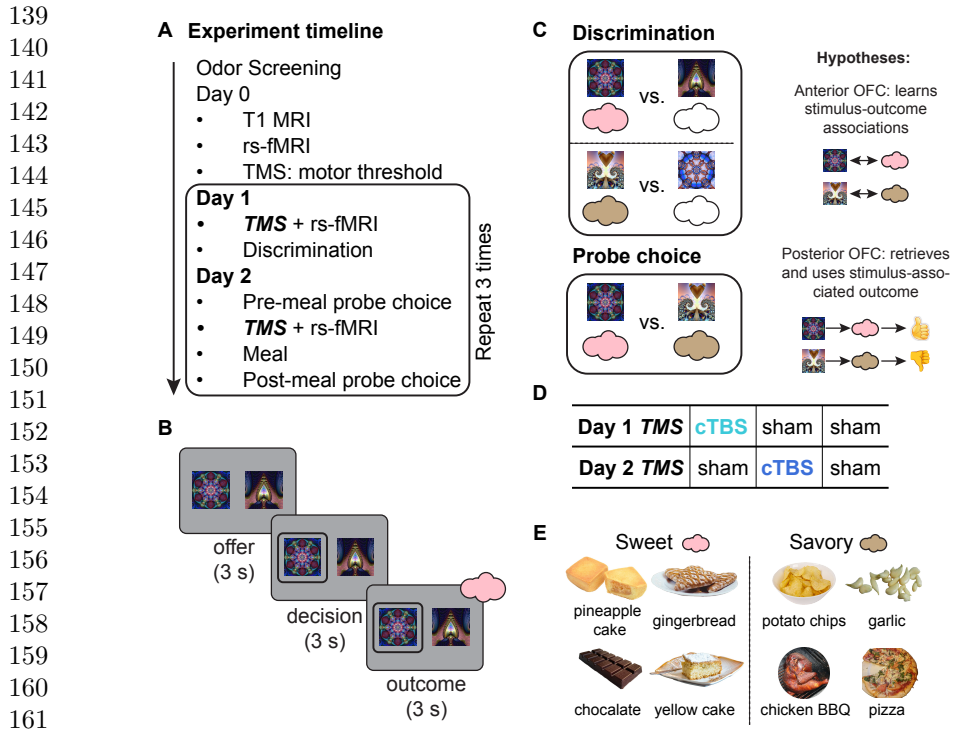


**Fig. 1: Experimental design and outcome devaluation task. A. Experiment timeline.** Following odor screening, participants completed T1 MRI, resting-state fMRI, and TMS motor threshold determination on Day 0. On Day 1, they received either continuous theta burst stimulation (cTBS) or sham TMS before a discrimination task. On Day 2, they performed a pre-meal free choice task, received TMS (cTBS or sham), consumed a meal, and then completed a post-meal free choice task. **B. Trial structure of discrimination and choice tasks.** Each trial started with an offer phase (3 s), presenting two visual stimuli paired with different outcomes, followed by a decision phase (maximum 3 s) where participants selected one stimulus. In the discrimination task, the trial concluded with an outcome phase (3 s) where participants received an odor or no odor, depending on their choice. **C. Task structure.** In the discrimination task, participants learned which stimuli predicted odors (colored clouds) versus non-odor (i.e., clean air, empty clouds) outcomes. In the free choice task, participants selected stimuli based on learned odor associations and their odor preference, but without immediate odor delivery. The free choice task also included trials comparing odor-predictive and non-odor-predictive stimuli, similar to the discrimination task. **D. TMS conditions.** Participants were assigned to one of three counterbalanced conditions: (1) cTBS on Day 1, sham on Day 2 (cTBS-sham), (2) sham on Day 1, cTBS on Day 2 (sham-cTBS), and (3) sham on both days (sham-sham). **E. Odor stimuli.** Eight food-related odors (savory and sweet). One savory and one sweet odor was selected per participant to match pleasantness ratings.

184

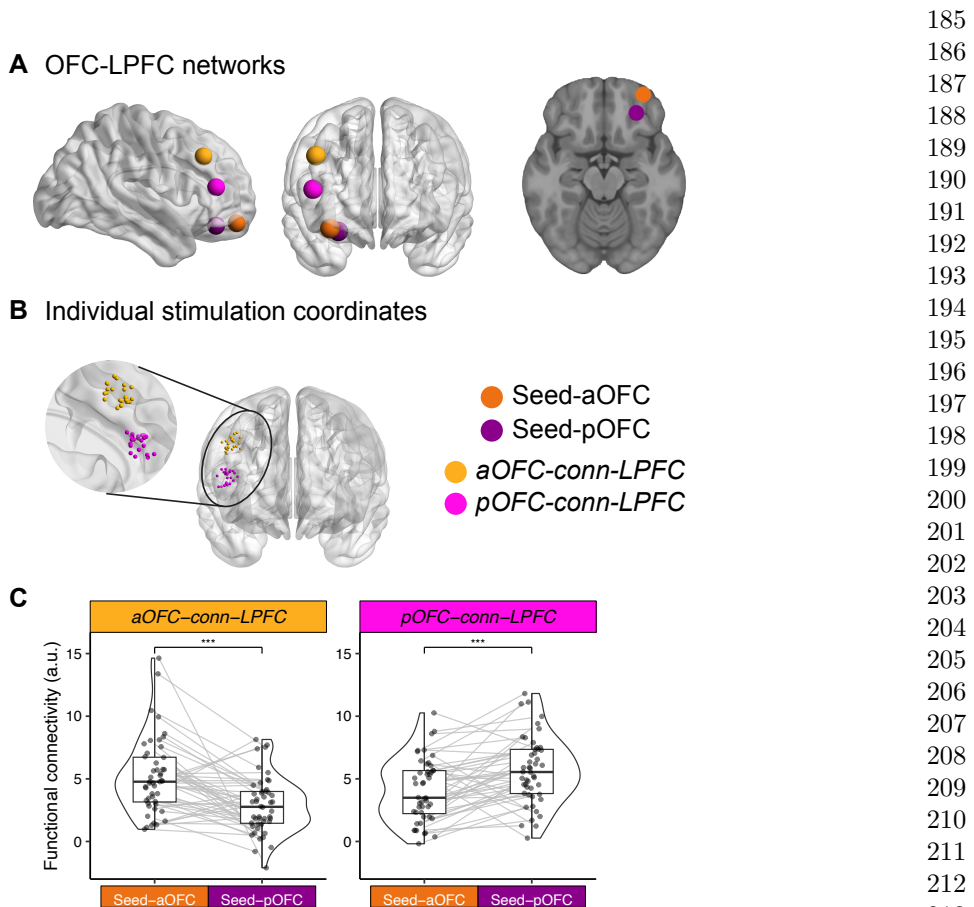


**Fig. 2: Network-targeted cTBS.** **A. OFC-LPFC networks.** Seed regions in the anterior (aOFC; tangerine, MNI coordinates: [34, 54, -14]) and posterior OFC (pOFC; magenta, MNI coordinates: [28, 38, -16]), along with their corresponding connectivity-based target regions in the lateral prefrontal cortex (LPFC), are shown on cortical surface renderings. Brain visualizations were generated using BrainNet Viewer (Xia et al, 2013), and the axial slice corresponds to  $z = -16$  in MNI space. **B. Individual stimulation coordinates.** LPFC stimulation sites were individually selected to maximize functional connectivity with either the aOFC or pOFC seed region. The zoomed view shows the distribution of stimulation coordinates across participants, color-coded by group. **C. Functional connectivity estimates.** Half-violin plots depict the distribution of resting-state functional connectivity between LPFC stimulation sites and each OFC seed region. Each dot represents an individual participant's connectivity estimate, and gray lines connect paired within-subject values across seed regions. Boxplots indicate the median and interquartile range. Asterisks denote significant differences between connectivity patterns ( $***p < 0.001$ ).

task on Day 1 or before the meal on Day 2 (Fig. 1A)—and targeted either the anterior (aOFC) or posterior (pOFC) portions of the lateral OFC in different groups of subjects (Fig. 2A). Stimulation targets were defined using MNI coordinates in the right hemisphere: aOFC at [34, 54, -14] and pOFC at [28, 38, -16]. Each target showed strong functional connectivity with isolated lateral prefrontal cortex (LPFC) ROIs (referred to as aOFC-conn-LPFC and pOFC-conn-LPFC, respectively). Based on resting-state fMRI data collected on Day 0, we individually selected LPFC stimulation sites with the highest connectivity to the respective aOFC or pOFC targets (Fig. 2B). We confirmed the functional separation of these networks across all resting-state fMRI sessions: the aOFC-conn-LPFC showed stronger connectivity with the aOFC than the pOFC ( $W = 988, p = 1.57e - 5$ , Wilcoxon signed rank test, two-sided), and the pOFC-conn-LPFC showed stronger connectivity with the pOFC than the aOFC ( $W = 936, p = 2.23e - 4$ ) (Fig. 2C).

244

## 245 2.2 Discrimination learning and selective satiation effects.

246

247 On Day 1, participants completed a discrimination task in which they selected, from  
248 pairs of stimuli, the one associated with desirable food odors (vs. clean air). Over  
249 five runs, they showed significant improvement in choosing odor-predictive stimuli,  
250 indicating successful value acquisition (Fig. 3A;  $p < 2.2 \times 10^{-16}$ ).

251 To evaluate the impact of selective satiation—induced by feeding participants an  
252 odor-matched meal—we first examined changes in rated odor pleasantness. There was  
253 a robust effect of selective satiation on the change in odor pleasantness ratings (post-  
254 meal minus pre-meal) ( $p = 2.75e - 13$ , Fig. 3B). Specifically, sated odors showed  
255 a larger decrease in pleasantness compared to non-sated ones. This reduction was  
256 unaffected by TMS condition (sham vs. cTBS, Day 2), stimulation target (aOFC  
257 vs. pOFC), session number (1<sup>st</sup>, 2<sup>nd</sup>, 3<sup>rd</sup>), or sated odor type (savory/sweet) (all  
258  $p > 0.05$ ; Extended Data Fig. 1). Consistent with previous findings (Izquierdo et al,  
259 2004; Rhodes and Murray, 2013; Howard et al, 2020), these results suggest that TMS  
260 did not impair participants’ ability to update the value of reward outcomes.

261 We then assessed behavioral evidence of selective satiation by analyzing choices  
262 between stimuli predictive of sated (SA) and non-sated (NS) odors in novel savory-  
263 sweet stimulus pairs not used during Day 1 training. Collapsing across sessions,  
264 participants made significantly fewer SA choices post-meal compared to pre-meal,  
265 both in the aOFC (Wilcoxon signed rank test, one-sided,  $p = 0.024$ ) and in the  
266 pOFC ( $p = 2.3e - 3$ ) groups (Fig. 3C), confirming an effect of selective satiation on  
267 probe choices. SA choices were significantly correlated with the pleasantness difference  
268 between sated and non-sated odors, both before and after the meal (Extended Data  
269 Fig. 2A, B), indicating that choices reflected relative odor preferences as expected.

270 To quantify the behavioral impact of subjective value change, we computed a  
271 “selective satiation index” by subtracting the change in pleasantness ratings for non-  
272 sated odors from those for sated odors (post-meal minus pre-meal). This index was  
273 significantly correlated with the corresponding change in SA choices (Pearson’s  $r =$   
274  $0.46, p = 8.3 \times 10^{-4}$ ; Extended Data Fig. 2C), further supporting a link between  
275 subjective devaluation and behavioral change.

276

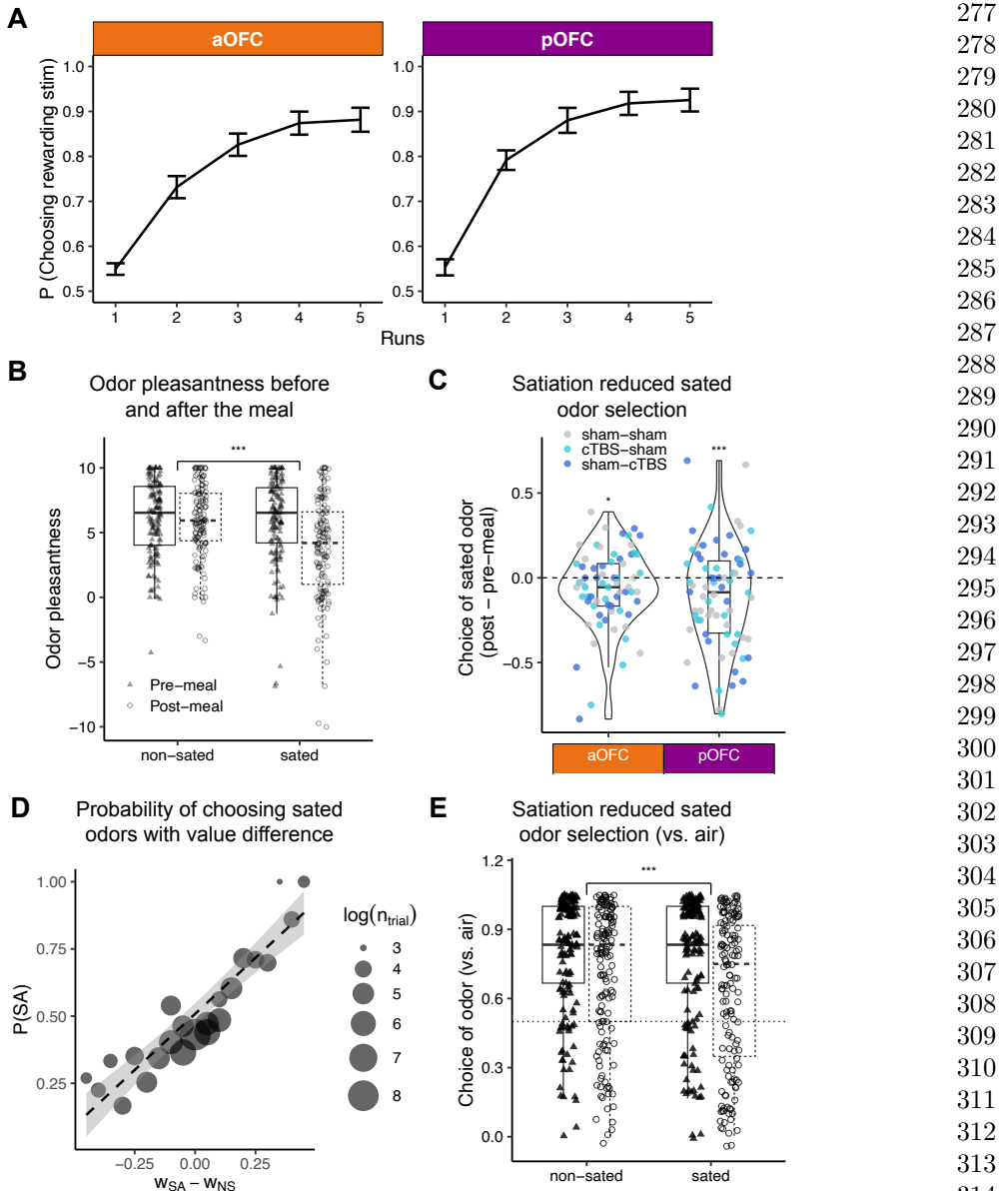


**Fig. 3: Discrimination learning and selective satiation effects.** **A.** Participants learned to select odor-predictive stimuli over five runs of the Day 1 discrimination task, shown separately for the aOFC and pOFC groups. **B.** Rated pleasantness of sated and non-sated odors before and after the meal. Pleasantness decreased significantly for sated odors post-meal, consistent with selective satiation. **C.** Change in choice proportion for sated odors in sweet–savory trials from pre- to post-meal, across three TMS conditions (sham–sham, light blue; cTBS–sham, dark blue; sham–cTBS), for both aOFC- and pOFC-targeted stimulation. **D.** Probability of choosing the sated odor stimulus as a function of the estimated value difference between the sated and non-sated options ( $w_{SA} - w_{NS}$ ). Dot size reflects the number of trials (log-scaled) at each value bin. **E.** Choice between odors and clean air, for sated and non-sated odors, before and after the meal. The p-value reflects a likelihood ratio test evaluating the interaction between odor type (sated vs. non-sated) and meal timing (pre vs. post), based on a trial-wise mixed-effects model.

323     Although not part of our original hypothesis—and rarely examined in outcome  
324 devaluation studies—we found that individual choices were also influenced by the  
325 learned value of each stimulus. Because learning on Day 1 was not perfect and likely  
326 varied across participants, sessions, and stimuli, we estimated individual stimulus val-  
327 ues to capture this variability (see Section 2.5 for details). The probability of choosing  
328 the SA over the NS option increased significantly with the value difference between  
329 the two stimuli ( $w_{SA} - w_{NS}$ ) (Pearson's  $r = 0.92$ ,  $p = 3.49e - 10$ ; Fig. 3D, Extended  
330 Data Fig. 2B). Accordingly, when evaluating the effects of cTBS (applied on Day 1  
331 or Day 2) on SA choices during Day 2, we included both the learned value difference  
332 ( $w_{SA} - w_{NS}$ ) and the selective satiation index as regressors to account for factors  
333 influencing behavior beyond the effects of TMS.

334     Finally, we analyzed participants' selections between stimuli where one predicted  
335 an odor and the other predicted clean air—pairings learned during the Day 1 discrim-  
336 ination task. Across sessions, participants showed a significant post-meal reduction in  
337 choosing odor-predictive stimuli ( $p < 2.2e - 16$ ), with a significantly greater reduction  
338 for stimuli predictive of the sated versus non-sated odor ( $p = 1.187e - 6$ ) (Fig. 3E).

339

### 340 **2.3 Posterior, but not anterior, OFC-targeted cTBS before the 341 free choice impairs outcome devaluation**

342

343     To examine the role of the aOFC and pOFC in outcome devaluation during the test  
344 phase, we focused on the “sham-sham” and “sham-cTBS” TMS conditions. We found  
345 a significant interaction between stimulation target (aOFC vs. pOFC) and TMS con-  
346 dition (sham vs. cTBS on Day 2, Day 1 fixed at sham) in predicting SA choices  
347 ( $p = 0.00548$ ), according to mixed-effects logistic models on post-meal SA choices,  
348 with the session odor preference baseline, satiation status, and the value difference  
349 ( $w_{SA} - w_{NS}$ ) accounted for. We further separately analyzed the aOFC and pOFC  
350 group (Fig. 4B) and found that cTBS significantly increased SA choices — indicat-  
351 ing poorer adaptation to the current goal — only in the pOFC group ( $p = 0.00034$ ),  
352 but not in the aOFC group ( $p = 0.655$ ). Additionally, we confirmed that the effect of  
353 pOFC-targeted cTBS on SA choices remained robust regardless of session order (??B).

354     We conducted additional analyses to assess whether the effect of TMS on SA  
355 choices was driven by other factors, such as satiation status or perceived TMS dis-  
356 comfort or intensity. The across-participant correlations between pleasantness ratings  
357 and SA choices were unchanged by Day 2 cTBS (all  $p > 0.05$ ; Extended Data Fig.  
358 2C), suggesting that the effect of Day 2 cTBS on SA choices was not modulated by  
359 satiation status. Moreover, the changes in SA choices induced by cTBS could not be  
360 explained by perceived TMS discomfort or intensity, as incorporating TMS ratings  
361 into the regression models did not alter any of the findings (Extended Data Fig. 4). We  
362 also examined participants' choices between an odor and clean air to assess potential  
363 TMS effects, but found no significant effects in either the aOFC or pOFC group.

364     Together, this suggests that pOFC-targeted cTBS before the free choice phase  
365 impaired outcome devaluation, as indicated by the continued selection of sated odor-  
366 predicting stimuli. In contrast, aOFC-targeted cTBS had no such effect, highlighting  
367 the specificity of the pOFC involvement.

368

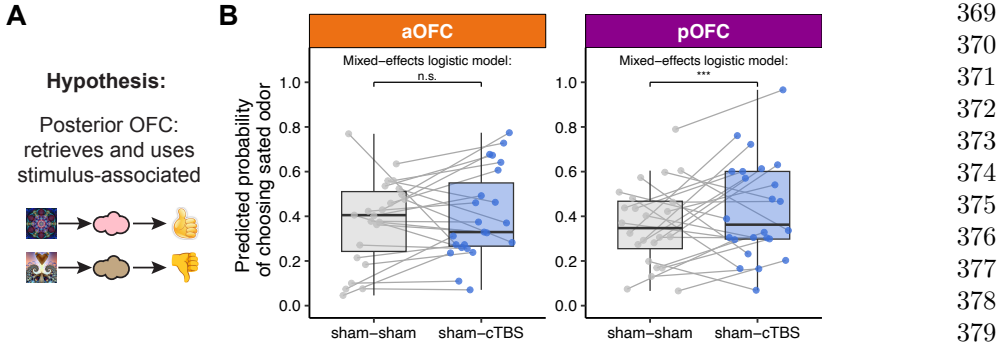
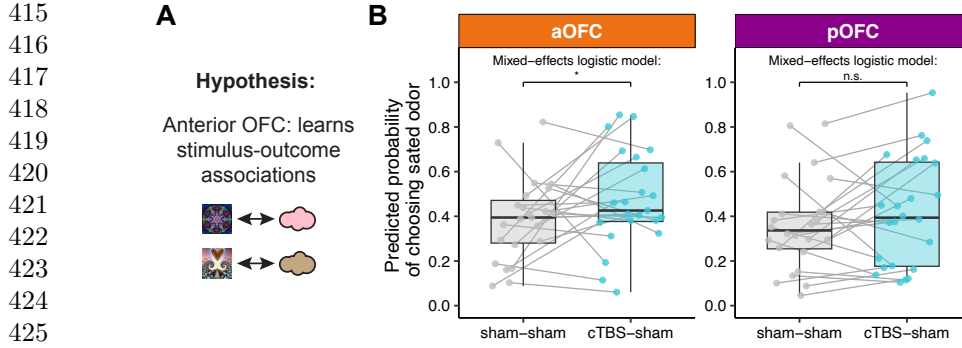


**Fig. 4: Posterior, but not anterior, OFC-targeted cTBS before the free choice impaired outcome devaluation.** **A.** Study hypothesis: the posterior OFC (pOFC) is involved in retrieving and using stimulus–outcome associations to guide choices. **B.** Model-predicted probability of choosing the sated odors under sham–sham and sham–cTBS conditions, shown separately for anterior (aOFC, tangerine) and posterior (pOFC, magenta) OFC-targeting groups. Each dot represents a participant’s average predicted probability, and gray lines connect values from the same participant across conditions. Box plots show group-level distributions of fitted values. Statistical comparisons were conducted using trial-wise mixed-effects logistic regression controlling for baseline odor preference, satiation status, and value difference between sated and non-sated options ( $w_{SA} - w_{NS}$ ). A significant increase in sated odor choice was observed following Day 2 pOFC cTBS (\*\*\*)<sup>3</sup>, but no effect in the aOFC group (n.s.).

## 2.4 Anterior, but not posterior, OFC targeted cTBS before discrimination learning impaired subsequent outcome devaluation

We explored whether cTBS targeting aOFC and pOFC before learning could affect outcome devaluation measured on Day 2, as would be expected if cTBS disrupted the latent learning of stimulus-reward identity associated during discrimination training (Fig. 5A).

To assess Day 1 cTBS effect on post-meal choices of sated odors on sweet-savory choices, we focused on “sham-sham” and “cTBS-sham” conditions. For the aOFC group, both TMS condition and session number significantly influenced post-meal sated odor choices, with a significant interaction between the two. Specifically, the cTBS-sham condition significantly increased the selection of sated odors (Fig. 5B;  $\hat{\beta} = 1.527$ , SE = 0.625,  $p = 0.015$ ), and this effect diminished over sessions ( $\hat{\beta} = -0.657$ , SE = 0.290,  $p = 0.024$ ). Choices also increased with session number ( $\hat{\beta} = 0.550$ , SE = 0.165,  $p = 8.5e - 5$ ). Similar to how we examined Day 2 effect, these effects were with the session odor preference baseline, satiation status, and the value difference ( $w_{SA} - w_{NS}$ ) accounted for, and those covariates were significant predictors. Overall, aOFC-targeted cTBS on Day 1 increased post-meal choices of stimuli predicting sated odors, with the effect moderated by session number.



426           **Fig. 5: Anterior, but not posterior, OFC-targeted cTBS on Day 1 impaired**  
427           **subsequent outcome devaluation.** **A.** Study hypothesis: the anterior OFC (aOFC)  
428           is involved in learning stimulus–outcome associations. **B.** Model-predicted probability  
429           of choosing the sated odor in the post-meal test, compared between sham–sham and  
430           cTBS–sham sessions, separately for anterior (aOFC, tangerine) and posterior (pOFC,  
431           magenta) targeting groups. Each dot represents a participant’s average predicted prob-  
432           ability, with gray lines connecting values from the same participant across conditions.  
433           Box plots indicate the group-level distribution of fitted values. Statistical compar-  
434           isons were conducted using trial-wise mixed-effects logistic regression, controlling for  
435           value difference, pre-meal odor preference, and selective satiation effects. A significant  
436           increase in sated odor choice was observed following Day 1 aOFC cTBS (\*), but no  
437           effect in the pOFC group (n.s.).

438

439

440           In contrast, similar analyses in the pOFC group revealed no significant difference  
441           between the sham-sham and cTBS-sham stimulation conditions (Fig. 5;  $p = 0.24$ ).  
442           Pre-meal odor preference and value difference were significant predictors of post-meal  
443           choices, while the selective satiation index was not ( $p > 0.05$ ). Additionally, no inter-  
444           action between stimulation targeted location (aOFC vs. pOFC) and TMS condition  
445           (sham-sham vs. cTBS-sham) was identified ( $p = 0.37$ ).

446           These findings support our hypothesis that the aOFC plays a critical role in learning  
447           the specific stimulus-outcome associations on Day 1, even when the task does not  
448           explicitly require it (i.e., latent learning). Notably, this result is independent of the  
449           Day 2 TMS, emphasizing the aOFC’s importance in constructing cognitive maps that  
450           are later used to guide behavior.

451

## 452           **2.5 Posterior and anterior, OFC-targeted cTBS disrupted** 453           **value acquisition during the first session**

454           As noted in section 2.2, participants showed significant improvement in selecting  
455           odor-predictive stimuli over five runs. A more detailed analysis revealed that this  
456           improvement was influenced by the TMS condition applied prior to the task (cTBS  
457           vs. sham;  $p = 1.27 \times 10^{-7}$ ), session number (1<sup>st</sup>, 2<sup>nd</sup>, 3<sup>rd</sup>;  $p = 1.71 \times 10^{-11}$ ), and their  
458

459

460

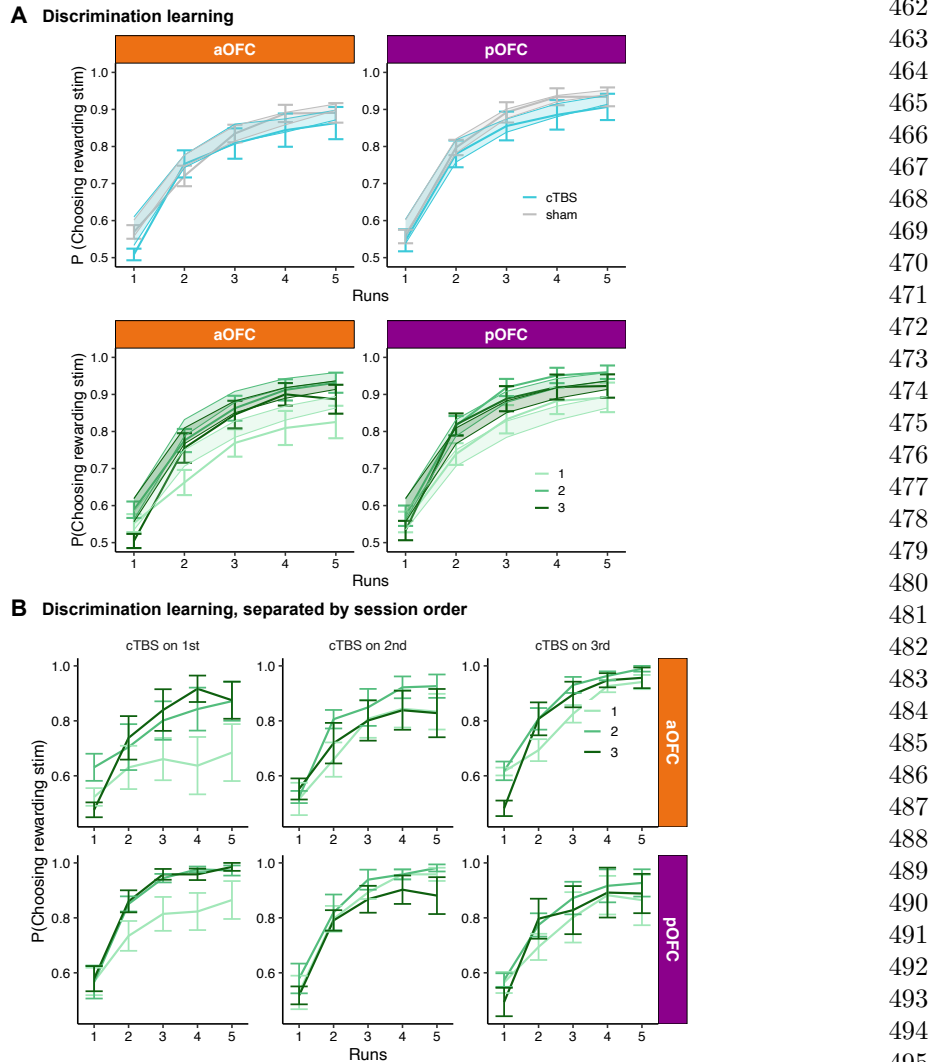


**Fig. 6: Posterior or anterior OFC-targeted cTBS disrupted value acquisition during the first session.** **A.** Discrimination accuracy over five runs during the Day 1 task, plotted by TMS condition (cTBS vs. sham), session number (1<sup>st</sup>, 2<sup>nd</sup>, 3<sup>rd</sup>), and stimulation target (aOFC vs. pOFC). Line plots with error bars represent observed data, while shaded regions indicate the 95% confidence intervals based on simulated accuracy using posterior estimates of individual learning rates. **B.** Discrimination accuracy across runs, separated by session number and the session order of cTBS administration—that is, whether cTBS was applied during the 1<sup>st</sup>, 2<sup>nd</sup>, or 3<sup>rd</sup> session of the three-session experiment.

507 interaction ( $p = 1.93 \times 10^{-5}$ ), based on logistic mixed-effects models with participant  
508 as a random effect (see line plot with error bars in Fig. 6A).

509 To further examine the effects of TMS condition and session number on discrimination learning,  
510 we grouped participants based on the session in which they received cTBS or sham stimulation on Day 1 (Fig. 6B). This analysis revealed that the impairment in discrimination due to cTBS was evident only when cTBS was administered  
511 during the first session ( $p < 2.2 \times 10^{-16}$ ). We also tested whether the effect differed by  
512 stimulation target (anterior vs. posterior OFC) but found no significant interaction or  
513 main effect related to target location (all  $p > 0.05$ ).

514 To quantify and compare the learning process, we fitted a Rescorla–Wagner model  
515 to participants' discrimination behavior using a hierarchical Bayesian framework  
516 (Myung et al., 2005) (see **Supplementary Note** for details). We evaluated three  
517 model variants: one with condition-specific learning rates (based on TMS condition:  
518 sham vs. cTBS on Day 1), one with session-specific learning rates (sessions 1, 2, and 3),  
519 and one with a fixed learning rate across all sessions and conditions. Model comparison  
520 using the deviance information criterion (DIC) (Spiegelhalter et al., 2002) indicated  
521 that the session-specific model provided the best fit (DIC: session-specific = 13,161.95;  
522 condition-specific = 13,544.84; fixed = 14,045.46). This model closely captured the  
523 observed data, as shown by the shaded fits in Fig. 6A.

524 Overall, cTBS targeting both posterior and anterior OFC impaired value acquisition  
525 in the discrimination task, but only when applied during the first session. This  
526 suggests a general disruptive effect of cTBS on participants' ability to perform the  
527 task when administered early. As noted in section 2.2, we incorporated the estimated  
528 difference in learned values as regressors when assessing the effects of Day 1 or Day 2  
529 cTBS on sated odor (SA) choices during Day 2.

530

### 531 3 Discussion

532

533 In this study, we used a three-session times two-day design with network-targeted TMS  
534 to selectively modulate activity in anterior and posterior subregions of the human  
535 lateral OFC. Using an outcome devaluation task requiring adaptive decision-making  
536 based on learned stimulus-outcome identity associations, we found that TMS targeting  
537 the pOFC (but not the aOFC) prior to the meal disrupted adaptive behavior,  
538 as evidenced by continued choices of stimuli predicting sated rewards in the probe  
539 test. Conversely, disrupting the aOFC (but not the pOFC) before learning stimulus-  
540 outcome associations on Day 1 also impaired behavior in the probe test on the following  
541 day. These findings demonstrate that the aOFC facilitates adaptive decision-making by  
542 supporting the acquisition of stimulus-outcome associations, while the pOFC supports  
543 their use.

544 Our findings suggest that the anterior OFC plays a key role in enabling individuals  
545 to learn specific stimulus-outcome structures (e.g., associating visual stimuli with spe-  
546 cific odors) even when the current task does not explicitly require it. This aligns with  
547 prior work indicating that the OFC represents the current task state (Wilson et al.,  
548 2014; Vaidya and Badre, 2022). However, stimulus-outcome associations in our study  
549 were directly observable, contrasting with only partially observable problems where  
550

states have to be inferred or retained in memory (e.g. Zhou et al, 2019; Schuck et al, 2016). The function of the anterior OFC in cognitive map construction identified here bears more resemblance to previous research indicating that both humans and animals are driven by curiosity to explore and learn about the environment, known as latent learning (Wang and Hayden, 2021; Tolman, 1948), constructing a representation of the world even in the absence of direct rewards (Wang and Hayden, 2021; O'keefe and Nadel, 1978; Kidd and Hayden, 2015). Such cognitive maps, once formed, provide a foundation for guiding goal-directed behaviors (Behrens et al, 2018; Tolman, 1948). Importantly, although discrimination training in our task involved reward, learning the specific identity of the reward was not required or reinforced. In that sense, our work parallels a previous study in rats showing that chemogenetic inhibition of lateral OFC caused a deficit in credit assignment during map construction (Costa et al, 2023). Notably, our findings highlight the specific and causal role of the anterior part of the lateral OFC in forming cognitive maps. This work is also in line with recent studies in both rodents and humans suggesting that the lateral OFC supports learning the identity of rewards associated with stimuli (Costa et al, 2023; Howard et al, 2015; Howard and Kahnt, 2018; Liu et al, 2024; McDannald et al, 2014; Namboodiri et al, 2019). However, the current study offers a novel and unique contribution by showing that aOFC remains essential even when individuals are not explicitly tasked with encoding such identity information. Moreover, the effect of disrupting learning of identity can be revealed in later stages, when the encoded information becomes crucial for adaptive decision making.

Consistent with previous work (Howard et al, 2020), we found that the posterior part of the lateral OFC is critical for goal-directed behavior during the probe test. Without an intact posterior OFC, individuals fail to change their choices after selective satiation, continuing to choose stimuli predicting devalued outcomes. This suggests that the posterior OFC may support retrieving and applying the cognitive map to guide current behavior. Importantly, our findings show that this effect is specific for the posterior OFC network and does not occur when stimulating a network centered on the adjacent anterior OFC. This provides important information on the specific roles of different OFC subregions and highlights the regional specificity of network-targeted TMS more generally.

Our findings align with a range of studies demonstrating distinct roles of OFC subregions across various tasks and across species, including goal-directed choices with outcome devaluation (Murray et al, 2015), two-choice probabilistic tasks (Stoll and Rudebeck, 2024), differential information encoding in the OFC (Rich and Wallis, 2017), and the specific contributions of lateral OFC subregions to economic decision-making (Wang et al, 2022). Particularly relevant is work in non-human primates examining the differential roles of OFC subregions in flexible behavior (Murray et al, 2015), demonstrating that the anterior OFC (area 11) is more involved in goal selection during choice, while the posterior OFC (area 13) primarily supports outcome value updating. In contrast to Murray et al (2015), our study focused on the differential involvement of lateral OFC subregions in learning and using stimulus-outcome identity associations to guide adaptive behavior. While a precise cross-species mapping of

599 our defined anterior and posterior OFC regions to animal models remains challenging  
600 our study is, to our knowledge, the first causal investigation to differentiate the  
601 functional roles of the human OFC along the anterior-posterior gradient. Recognizing  
602 these functional differences represents a substantial advance in our understanding of  
603 this brain area and will help guide future studies assessing the role of OFC in learning  
604 and decision-making. In human subjects research, this distinction is particularly  
605 important for neuroimaging studies and neuromodulation approaches targeting the  
606 OFC (Howard and Kahnt, 2021; Howard et al, 2020; Liu et al, 2024; Wang et al, 2020;  
607 Tegelbeckers et al, 2023; Ouellet et al, 2015).

608 Although not part of our initial hypothesis, we found that cTBS targeting both  
609 the anterior and posterior OFC disrupted performance in the discrimination task, but  
610 only during the first session, with no impact in later sessions. This challenges the  
611 view that OFC is not important for simple Pavlovian acquisition (Murray et al, 2007;  
612 Delamater, 2007; Stalnaker et al, 2014), in line with recent rodent studies suggesting  
613 that OFC's role in Pavlovian acquisition may be more nuanced than previously thought  
614 (Panayi and Killcross, 2021). Interpreting this result is further complicated by our  
615 within-participant design, as the deficit emerged only in the first session. This initial  
616 impairment likely reflects difficulty in grasping the basic task structure. Once this  
617 fundamental task structure was learned, it could be reused in subsequent sessions  
618 with different stimulus sets (Behrens et al, 2018; Harlow, 1949), potentially explaining  
619 why TMS had no effect on task performance in later sessions. To account for these  
620 effects, we included the stimulus-level learned values of each option in the analysis of  
621 SA choices, instead of simply assuming “perfect” learning during the discrimination  
622 learning task (Murray et al, 2015; Howard et al, 2020).

623 One limitation of this study is the within-participant design, which enhances sta-  
624 tistical power but may introduce interpretive challenges. For instance, participants  
625 completing the first session could learn that odor identity would be relevant for the  
626 Day 2 task, potentially altering their approach to processing odor identity in later ses-  
627 sions. To test this possibility, we compared groups of participants based on the order of  
628 cTBS and sham stimulation. Importantly, our findings were not driven by stimulation  
629 order, speaking to the robustness of our results. However, the small sample size within  
630 each session-order group may limit the ability to detect subtle order effects. Another  
631 limitation is the difference in perceived TMS discomfort and intensity between cTBS  
632 and sham conditions as reported in the current work and our previous work (Liu et al,  
633 2024). However, we found no differences in these ratings between anterior and posterior  
634 sites, and individual differences did not account for the observed behavioral effects.  
635

## 636 4 Conclusion

637

638 In conclusion, our study reveals distinct roles of the anterior and posterior OFC net-  
639 work in cognitive map formation and its use for goal-directed behavior in humans.  
640 These findings contribute to a better understanding of the functional role of OFC sub-  
641 regions in adaptive decision-making. Additionally, this work offers valuable insights  
642 for research in rodents and non-human primates, advancing our understanding of the  
643 neural mechanisms underlying adaptive decision-making across species.  
644

<b>5 Methods</b>	645
<b>5.1 Participants</b>	646
Eighty-eight healthy, right-handed participants (ages 18-40) with no history of psychiatric or neurological disease provided written informed consent to participate in this study. Of these, 48 participants (16 males; ages 18-40, mean = 25.17, SD = 4.14) completed all sessions. Due to a technical error, behavioral data from the cTBS-sham session were unavailable for one participant in the posterior targeting group (see section 5.2); however, data from the other two sessions were included in the analysis where applicable. MRI data for five resting-state scans were not acquired and excluded from analysis. All participants fasted for at least four hours before each study visit.	647
	648
	649
	650
	651
	652
	653
	654
	655
	656
	657
	658
<b>5.2 Study design</b>	659
The study consisted of eight visits (Fig. 1A, D), with Day 1 and Day 2 occurring on consecutive days. The two-day experiment was repeated across three sessions. Sessions were spaced at least one week apart, with a median interval of 13.5 days, a mean of 18.02 days (SD = 9.09), and a range of 7 to 63 days. On each Day 1 and Day 2, participants received either continuous theta-burst stimulation (cTBS, labeled C) or sham stimulation (S). Over the three sessions, they experienced three TMS conditions: cTBS-sham (CS), sham-cTBS (SC), and sham-sham (SS). The order of these conditions was counterbalanced, with 9 participants receiving CS-SC-SS, 7 receiving CS-SS-SC, and the remaining 32 equally assigned to one of the other four possible sequences (SC-CS-SS, SC-SS-CS, SS-CS-SC, and SS-SC-CS).	660
	661
	662
	663
	664
	665
	666
	667
	668
	669
	670
	671
	672
	673
	674
	675
	676
	677
	678
	679
<b>5.3 Screening session</b>	680
After providing informed consent and completing eligibility screening, participants rated the pleasantness of eight food odors. These odors, supplied by International Flavors and Fragrances (New York, NY), included four savory (garlic, potato chip, pizza, barbecue) and four sweet (chocolate, yellow cake, pineapple cake, gingerbread) odors. In each trial, participants smelled a food odor for 2 seconds and rated their liking on a visual analog scale ranging from “Most Disliked Sensation Imaginable” to “Most Liked Sensation Imaginable.” Ratings were made using a scroll wheel and keyboard press. Each odor was presented three times in a pseudo-randomized order, and ratings were averaged per odor. Based on these ratings, two odors (one savory, one sweet) that were pleasant (above neutral) and closely matched were selected for	681
	682
	683
	684
	685
	686
	687
	688
	689
	690

691 the discrimination and choice tasks. These odors were used across all three sessions.  
692 Participants were excluded if no suitable odors were identified.

693 A custom-built, computer-controlled olfactometer was used to deliver the odors  
694 with precise timing to nasal masks worn by participants. The olfactometer directed  
695 medical-grade air through the headspace of amber bottles containing the odor solu-  
696 tions at a constant flow rate of 3.2L/min. Using two independent mass flow controllers  
697 (Alicat, Tucson, AZ), the device enabled precise dilution of the odorized air with odor-  
698 less air. Throughout the experiment, a constant stream of odorless air was delivered,  
699 and odorized air was mixed in at specific time points without altering the overall flow  
700 rate or causing somatosensory stimulation.

701

#### 702 **5.4 Day 0: Scan & Motor threshold**

703

704 We acquired a T1-weighted structural MRI scan to assist with TMS neuronavigation  
705 and an 8 min multi-echo resting-state fMRI scan (310 volumes, TR = 1.5s) to individ-  
706 ually define the OFC-targeted cTBS coordinates (see section 5.8). The same scanning  
707 parameters were used for other resting-state scans. We then measured resting motor  
708 threshold (rMT) by administering single TMS pulses to the hand area of the left motor  
709 cortex. rMT was defined as the lowest stimulator output required to evoke 5 visible  
710 thumb movements from 10 pulses.

711

#### 712 **5.5 Day 1: Discrimination task**

713

714 Participants first underwent a TMS session (cTBS or sham, see section 5.9) followed  
715 by a resting-state scan. Then they completed five runs of a discrimination task. In each  
716 trial, participants chose between two fractal stimuli: one associated with a savory or  
717 sweet odor, and the other with clean air. Stimuli were displayed for 3 seconds, followed  
718 by a choice phase (maximum 3 seconds). If participants selected a stimulus leading to  
719 an odor, the odor was delivered for 2 seconds. The inter-trial interval ranged from 4  
720 to 8 seconds. Each run consisted of 24 trials, using four groups of stimulus pairs: two  
721 sets (A and B) crossed with sweet/savory odors. Each combination had three non-  
722 overlapping stimulus pairs, resulting in 24 distinct fractals. Each pair was presented  
723 twice to counterbalance left and right positions on the screen. Choice and response  
724 times were recorded for each trial, and different fractals were used across the three  
725 sessions.

726

#### 727 **5.6 Day 2: Meal consumption and free choice task**

728

729 Day 2 started with an odor pleasantness rating followed by a choice task (pre-meal)  
730 where participants selected between pairs of stimuli. Afterwards, participants under-  
731 went a TMS session and then had a meal carefully matched in flavor to either the  
732 sweet or savory food odor used in their task. Following the meal, participants com-  
733 pleted another set of odor pleasantness ratings and the post-meal free choice task.  
734 Both pre-meal and post-meal choice tasks instructed participants to choose based on  
735 their current odor preferences.

736

The pre-meal free choice task included 30 trials, all from set A, consisting of 3  
sweet vs. clean air pairs, 3 savory vs. clean air pairs, and 9 savory vs. sweet pairs. Each

pair was presented twice to counterbalance left and right positions on the screen. The post-meal choice task included 60 trials from both sets A and B. In both pre- and post-meal choice tasks, similar to the discrimination task, every trial began with a pair of stimuli presented for 3 seconds, followed by a decision phase of up to 3 seconds. In the pre-meal free choice task, if participants selected a stimulus linked to an odor, the odor was delivered for 2 seconds after their choices. No odors were delivered during the post-meal free choice task. Participants received the odors chosen in five randomly selected trials at the end of the task. The inter-trial interval ranged from 4 to 8 seconds, and choice and response times were recorded from all trials. Pre- and post-meal free choices for both set A and set B stimuli were highly correlated ([Extended Data Fig. 3](#)), indicating consistent choices across sets based on odor preferences. Thus, to assess the satiation effect on choices, we used the pre-meal average choice from set A as a session-wise odor preference baseline and compared it with the post-meal choices.

## 5.7 MRI data acquisition

MRI data were acquired on a Siemens 3T PRISMA system equipped with a 64-channel head-neck coil. Each TMS session on Day 1 and Day 2 was immediately followed by a resting-state MRI scan. Resting-state fMRI data were collected across all seven sessions with the same multi-echo sequence (310 volumes; TR = 1.5s; TE1-TE3 = 14.60ms, 39.04ms, 63.48ms). The short TE of the first echo is beneficial to mitigate signal dropout near the OFC, as demonstrated in previous studies using both resting-state and task-based fMRI ([Fernandez et al, 2017](#); [Poser et al, 2006](#); [Kirilina et al, 2016](#); [Zhao et al, 2024](#)). Other scanning parameters included: flip angle, 72°, slice thickness, 2mm (no gap), multi-band acceleration factor 4, 60 slices with interleaved acquisition, matrix size 104 x 104 voxels, and field of view 208mm x 208mm. A 1mm isotropic T1-weighted structural scan was acquired on Day 0 session for neuronavigation during TMS and to aid spatial normalization.

## 5.8 Coordination selection for network-targeted TMS

The stimulation coordinates were computed based on the multi-echo resting-state MRI data collected from the Day 0 session. We defined our stimulation targets in the right hemisphere's aOFC and pOFC using MNI coordinates: aOFC [34, 54, -14] and pOFC [28, 38, -16]. The pOFC coordinates were identical to those used in our previous network-targeted TMS studies ([Howard et al, 2020](#); [Liu et al, 2024](#); [Wang et al, 2020](#); [Tegelbeckers et al, 2023](#)). Each targeted coordinate in the aOFC and pOFC exhibited strong functional connectivity with isolated clusters in the LPFC with peak coordinates of [44, 28, 38] and [46, 38, 14], respectively, as determined in data from Neurosynth.org involving a sample of 1,000 subjects.

We first generated spherical masks of 8-mm radius around these four coordinates in MNI space, each inclusively masked by the gray matter tissue probability map provided by SPM12 (thresholded at > 0.1). We then transformed these four masks to each subject's native space using the inverse deformation field generated during the normalization of the T1 anatomical image. We then specified two resting-state fMRI functional connectivity analyses (one per region) for each subject, using individual

783 aOFC and pOFC masks as the seed regions and motion parameters from the realign-  
784 ment of the first echo as regressors of no interest. Finally, stimulation coordinates were  
785 defined as the voxels within the right LPFC masks with the strongest functional con-  
786 nectivity to the right aOFC and pOFC seed regions, respectively. We used infrared  
787 MRI-guided stereotactic neuronavigation (LOCALITE) to apply stimulation to these  
788 two individual LPFC coordinates.

789

### 790 **5.9 Transcranial magnetic stimulation**

791

792 Similar to our previous work, the target coordinates were defined as the locations  
793 in the right LPFC with the strongest functional connectivity with the corresponding  
794 right OFC seed regions (see details above). The Figure-eight coil was tilted so that  
795 its long axis was approximately perpendicular to the long axis of the middle frontal  
796 gyrus. TMS was administered at 80% of the rMT using a cTBS protocol. This protocol  
797 involved delivering bursts of three pulses at 50 Hz every 200 ms (5 Hz) for a total of  
798 600 pulses over approximately 40 seconds. Stimulation was applied using a MagPro  
799 X100 stimulator equipped with a MagPro Cool-B65 A/P butterfly coil (MagVenture).  
800 Previous work has demonstrated that this cTBS protocol at 80% MT has inhibitory  
801 aftereffects which persist for 50–60 min over primary motor cortex (Huang et al,  
802 2005). Whereas cTBS was delivered by positioning the active side of the A/P coil to  
803 modulate neural tissue, sham cTBS was applied with the placebo side of the A/P coil,  
804 producing similar somatosensory and auditory experiences for the participant without  
805 modulating neural tissue. Electrodes were placed on participants' forehead and direct  
806 current stimulation was applied in synchrony with the TMS pulses to mask TMS  
807 effects and enhance the similarity between cTBS and sham sessions.

808 Participants were informed about potential muscle twitches in the face, eyes, and  
809 jaw during simulation. To assess tolerability, two single pulses were applied over the  
810 stimulation coordinates before administering cTBS. Discomfort and perceived stimula-  
811 tion intensity were evaluated after each TMS session. The cTBS sessions were generally  
812 rated as more uncomfortable and intense compared to the sham sessions. On a scale  
813 from 0 (not uncomfortable at all) to 10 (extremely uncomfortable), mean discomfort  
814 ratings were 3.38 for sham and 5.8 for cTBS sessions ( $p = 2.2e - 16$ , linear mixed  
815 effects model). Similarly, on a scale from 0 (not strong at all) to 10 (extremely strong),  
816 mean intensity ratings were 3.79 for sham and 6.23 for cTBS sessions ( $p = 2.2e - 16$ ,  
817 linear mixed effects model). Discomfort and intensity ratings did not differ between  
818 aOFC- or pOFC-targeted cTBS (all  $p > 0.6$ ). For analyses involving cTBS effects (Day  
819 1 or Day 2 TMS), standardized discomfort and intensity ratings were used to exam-  
820 ine correlations or regressions against other variables, assessing if the observed cTBS  
821 effects were driven by subjective discomfort or perceived TMS intensity, but none of  
822 the effects can be explained by those ratings (see [Extended Data Fig. 4](#)).

823

### 824 **5.10 Meal consumption**

825

826 On Day 2, participants consumed a meal following the TMS session to selectively  
827 satiate one of the two food odors. The meal items were carefully chosen to closely match  
828 the corresponding food odors, and water was provided. Participants were instructed

to eat until they felt very full and were then left alone for 15 minutes. Immediately afterward, they rated the pleasantness of the odors and proceeded to the post-meal choice task. On average, participants consumed  $669.89 \pm 44.16$  calories (SEM). Before analyzing the relationship between odor ratings and task behavior, we standardized the ratings within each participant across sessions. 829  
830  
831  
832  
833  
834

## 5.11 Multi-echo MRI data processing 835

Preprocessing of the multi-echo resting-state fMRI data involved several steps. First, all functional images from the smallest echo across all rs-fMRI runs were realigned to the first volume of the first echo, and the resulting voxel-to-world mapping matrix was applied to the other two echoes, volume by volume. All functional images were then resliced for each echo. Next, the images across the three echoes were combined using temporal signal-to-noise ratio (tSNR) weighting, following parallel-acquired inhomogeneity desensitized (PAID) approach (Poser et al, 2006). Specifically, voxel-wise tSNR maps were computed for each echo, multiplied by the echo time (TE), and normalized across the three echoes to generate weight maps. These weight maps were then used to combine the resliced images by multiplying each volume by its respective weight map. Lastly, the combined data underwent coregistration, normalization, and smoothing using a 6 mm FWHM Gaussian kernel. 836  
837  
838  
839  
840  
841  
842  
843  
844  
845  
846  
847  
848

## 5.12 Analysis of odor pleasantness rating 849

Odor pleasantness ratings (Figure 3A) were collected on a raw scale from -10 to 10. For statistical analyses, ratings were z-scored within each participant to account for individual differences in scale use. To evaluate whether selective satiation specifically reduced the pleasantness of the sated odor, we calculated the change in pleasantness (`PleasantChange`, defined as post-meal minus pre-meal) for each odor and session. We then fit two linear mixed-effects models with random intercepts for participants. The null model (`MPC0`) included only a random intercept, while the full model (`MPC1`) included an additional fixed effect of (`IsSated`), a binary variable indicating whether the odor was the sated one. Model comparison was performed using a likelihood ratio test. 850  
851  
852  
853  
854  
855  
856  
857  
858  
859  
860  
861  
862

```
MPC0 <- lmer(PleasantChange ~ (1 | Ppt), data = pc_data)
MPC1 <- lmer(PleasantChange ~ IsSated + (1 | Ppt), data = pc_data)
```

We then computed a session-wise index of the selective satiation effect, `SatIdx`, defined as the difference in `PleasantChange` between sated and non-sated odors. To explore whether this effect was influenced by additional factors — such as TMS condition (Day 2; sham vs. cTBS), TMS target site (aOFC vs. pOFC), session number (1<sup>st</sup>, 2<sup>nd</sup>, 3<sup>rd</sup>), or sated odor type (savory/sweet) — we fit a second set of linear mixed-effects models. Each model included one of these predictors and was compared against the same null model `MSatIdx0`. For example, to test the influence of TMS condition (`TMScond`), we fit and compared the following models: 863  
864  
865  
866  
867  
868  
869  
870  
871  
872  
873

```
MSatIdx0 <- lmer(SatIdx ~ (1 | Ppt), data = SatIdxDat)
MSatIdx1 <- lmer(SatIdx ~ TMScond + (1 | Ppt), data = SatIdxDat)
```

All mixed-effects models were fit using the `lme4` package in R. 874

875 **5.13 Analysis of Day 2 probe choices**

876 We analyzed the Day 2 probe choice data on sweet–savory choices, and split these  
877 analyses by TMS target site (aOFC and pOFC groups). As noted in Section 5.6,  
878 we used the pre-meal average choice for each session as a baseline measure of odor  
879 preference BasePref. Post-meal choices were baseline-corrected, and a one-sided  
880 Wilcoxon signed-rank test was performed, collapsed across sessions, to test for an  
881 overall reduction in preference for the sated odor due to selective satiation (Fig. 3B).  
882

883 To assess the effect of Day 2 TMScond (Day 2; sham vs. cTBS) on choices involving  
884 the sated odor, we analyzed the trial-wise data using logistic mixed-effects modeling.  
885 The models included the following covariates: (1) BasePref, the pre-meal baseline  
886 preference; (2) SatIdx, the session-wise reduction in pleasantness of the sated odor;  
887 and (3) ValueDiff, the value difference between the two choice options on each trial,  
888 reflecting discrimination learning from Day 1 (see Section 5.14). For each target group  
889 (aOFC and pOFC), we compared a full model (Mchoice1) that included the TMS  
890 condition (TMScond) with a reduced model (Mchoice0) that did not:  
891

```
Mchoice1 <- glmer(Choice ~ TMScond + ValueDiff + SatIdx + BasePref  
+ (1|Ppt), data = ChoiceDat, family = 'binomial')  
Mchoice0 <- glmer(Choice ~ ValueDiff + SatIdx + BasePref + (1|Ppt),  
data = ChoiceDat, family = 'binomial')
```

892 In these models, Choice was a binary outcome indicating whether the participant  
893 chose the sated odor (1) or the non-sated odor (0). To further examine whether  
894 the effect of TMS condition varied by stimulation site, we tested an additional model  
895 that included an interaction term between TMScond and TMStarget. We used the  
896 fitted function in R to extract trial-level predicted choices based on the best-fitting  
897 model for each group. These predicted values were then averaged within each participant  
898 to estimate the model-derived probability of choosing the sated odor, as shown  
899 in Fig. 4. The Day 1 TMS effect was analyzed in a similar manner, using the contrast  
900 between Day 1 sham and cTBS while holding Day 2 TMS constant at sham, as shown  
901 in Fig. 5.

902 **5.14 Analysis and modeling of discrimination learning**

903 We examined whether participants improved their performance across runs by fitting  
904 the following mixed-effects logistic regression models:  
905

```
Mdisc1 <- glmer(OdorChosen ~ Run + (1|Ppt), data = disc_dat, family  
= 'binomial')  
Mdisc0 <- glmer(OdorChosen ~ (1|Ppt), data = disc_dat, family =  
'binomial')
```

906 In these models, OdorChosen indicates whether the odor-predictive stimulus was  
907 selected (yes = 1), and Run ranges from 1 to 5. To assess learning across runs, we  
908 compared a full model (Mdisc1) that included Run as a fixed effect with a reduced  
909 model (Mdisc0) that did not.  
910

911 To further characterize learning, we employed a standard Rescorla-Wagner model  
912 (Rizley and Rescorla, 1972) to describe how participants acquired associations in  
913 the discrimination task. On each trial, participants chose between two stimuli: one  
914

predictive of an odor and the other predictive of clean air. Because stimulus pairs did not overlap across trials, we assumed that learning was primarily driven by the odor-predictive stimulus.	921 922 923
Accordingly, we modeled the learned value $w$ of the odor-predictive stimulus across trials. The model updated this value based on the prediction error, defined as the difference between the actual outcome ( $w = 1$ ) and the expected value. The learning rate determined how quickly $w$ was adjusted. All values were initialized at $w = 0.5$ , with $w = 1$ indicating complete acquisition.	924 925 926 927 928
For a given stimulus pair, when it was presented on trial $i$ , the value $w$ was updated as follows:	929 930 931 932
$w_{i+1} = w_i + \alpha \cdot (1 - w_i),$	933 934 935 936 937
where $\alpha$ denotes the learning rate for that stimulus pair on the current trial. We estimated a separate learning rate for each odor-predictive stimulus using a hierarchical Bayesian framework (Myung et al, 2005), with session-wise or condition-wise priors. This approach enabled us to derive individualized value trajectories for each odor-predictive stimulus, which were subsequently used in the analysis of probe choices on Day 2. Further details on model specification and estimation procedures are provided in the <b>Supplementary Text</b> . Hierarchical Bayesian modeling was implemented in R using the Rjags package.	938 939 940 941 942 943 944 945 946
<b>Acknowledgements.</b> We thank Dr. Yihong Yang for helpful discussions. This work was supported by National Institute on Deafness and Other Communication Disorders grant R01DC015426 (to T.K.) and the Intramural Research Program at the National Institute on Drug Abuse (ZIA DA000642, to T.K.). The opinions expressed in this work are the authors' own and do not reflect the view of the NIH/DHHS.	947 948 949 950 951 952 953
<b>6 Extended Data</b>	954 955 956 957
<b>References</b>	958 959 960 961 962 963 964 965 966
Balleine BW, Dickinson A (1998) Goal-directed instrumental action: contingency and incentive learning and their cortical substrates. <i>Neuropharmacology</i> 37(4-5):407–419	951 952 953
Baxter MG, Parker A, Lindner CC, et al (2000) Control of response selection by reinforcer value requires interaction of amygdala and orbital prefrontal cortex. <i>Journal of Neuroscience</i> 20(11):4311–4319	954 955 956 957
Behrens TE, Muller TH, Whittington JC, et al (2018) What is a cognitive map? organizing knowledge for flexible behavior. <i>Neuron</i> 100(2):490–509	958 959 960
Colwill RM, Rescorla RA (1985) Postconditioning devaluation of a reinforcer affects instrumental responding. <i>Journal of experimental psychology: animal behavior processes</i> 11(1):120	961 962 963 964
Costa KM, Scholz R, Lloyd K, et al (2023) The role of the lateral orbitofrontal cortex in creating cognitive maps. <i>Nature neuroscience</i> 26(1):107–115	965 966

- 967 Critchley HD, Rolls ET (1996) Hunger and satiety modify the responses of olfactory  
968 and visual neurons in the primate orbitofrontal cortex. *Journal of neurophysiology*  
969 75(4):1673–1686
- 970
- 971 Daw ND, Niv Y, Dayan P (2005) Uncertainty-based competition between pre-  
972 frontal and dorsolateral striatal systems for behavioral control. *Nature neuroscience*  
973 8(12):1704–1711
- 974
- 975 Delamater AR (2007) The role of the orbitofrontal cortex in sensory-specific encoding  
976 of associations in pavlovian and instrumental conditioning. *Annals of the New York  
977 Academy of Sciences* 1121(1):152–173
- 978
- 979 Fernandez B, Leuchs L, Sämann PG, et al (2017) Multi-echo epi of human fear  
980 conditioning reveals improved bold detection in ventromedial prefrontal cortex.  
981 *Neuroimage* 156:65–77
- 982
- 983 Gallagher M, McMahan RW, Schoenbaum G (1999) Orbitofrontal cortex and rep-  
984 resentation of incentive value in associative learning. *Journal of Neuroscience*  
985 19(15):6610–6614
- 986
- 987 Gardner MP, Schoenbaum G (2021) The orbitofrontal cartographer. *Behavioral  
988 neuroscience* 135(2):267
- 989
- 990 Gottfried JA, O'Doherty J, Dolan RJ (2003) Encoding predictive reward value in  
991 human amygdala and orbitofrontal cortex. *Science* 301(5636):1104–1107
- 992
- 993 Harlow HF (1949) The formation of learning sets. *Psychological review* 56(1):51
- 994
- 995 Heilbronner SR, Rodriguez-Romaguera J, Quirk GJ, et al (2016) Circuit-based corti-  
996 costriatal homologies between rat and primate. *Biological psychiatry* 80(7):509–521
- 997
- 998 Howard JD, Kahnt T (2017) Identity-specific reward representations in orbitofrontal  
999 cortex are modulated by selective devaluation. *Journal of Neuroscience* 37(10):2627–  
2638
- 1000
- 1001 Howard JD, Kahnt T (2018) Identity prediction errors in the human midbrain update  
1002 reward-identity expectations in the orbitofrontal cortex. *Nature communications*  
1003 9(1):1611
- 1004
- 1005 Howard JD, Kahnt T (2021) Causal investigations into orbitofrontal control of human  
1006 decision making. *Current opinion in behavioral sciences* 38:14–19
- 1007
- 1008 Howard JD, Gottfried JA, Tobler PN, et al (2015) Identity-specific coding of future  
1009 rewards in the human orbitofrontal cortex. *Proceedings of the National Academy  
1010 of Sciences* 112(16):5195–5200
- 1011
- 1012 Howard JD, Reynolds R, Smith DE, et al (2020) Targeted stimulation of  
human orbitofrontal networks disrupts outcome-guided behavior. *Current Biology*

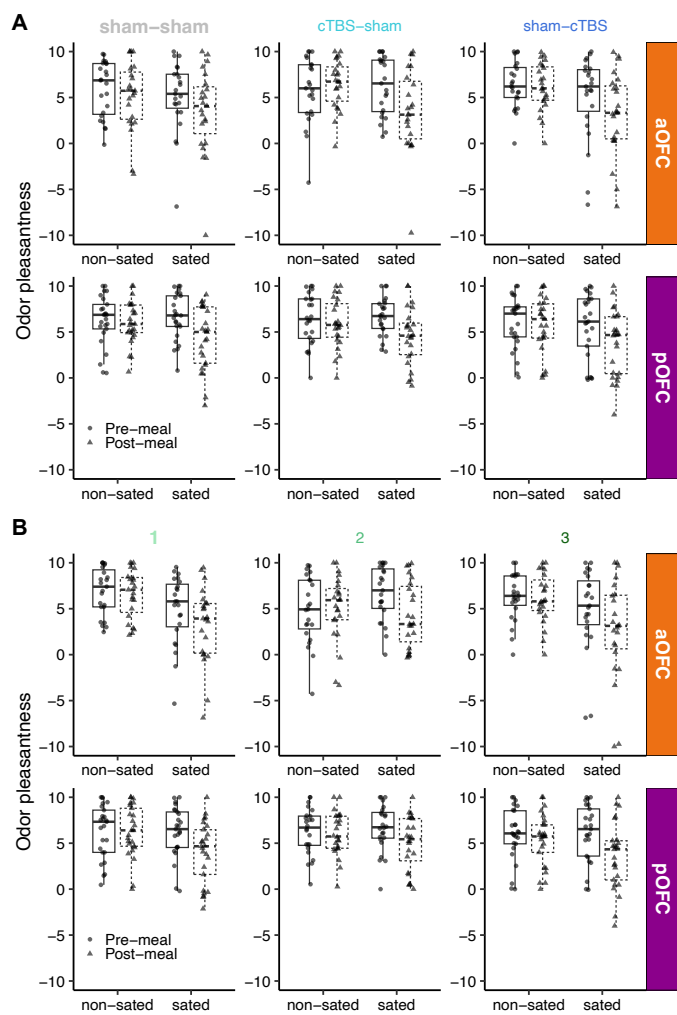
30(3):490–498	1013
Huang YZ, Edwards MJ, Rounis E, et al (2005) Theta burst stimulation of the human motor cortex. <i>Neuron</i> 45(2):201–206	1014
Izquierdo A (2017) Functional heterogeneity within rat orbitofrontal cortex in reward learning and decision making. <i>Journal of Neuroscience</i> 37(44):10529–10540	1015
Izquierdo A, Suda RK, Murray EA (2004) Bilateral orbital prefrontal cortex lesions in rhesus monkeys disrupt choices guided by both reward value and reward contingency. <i>Journal of Neuroscience</i> 24(34):7540–7548	1016
Kahnt T, Chang LJ, Park SQ, et al (2012) Connectivity-based parcellation of the human orbitofrontal cortex. <i>Journal of Neuroscience</i> 32(18):6240–6250	1017
Kidd C, Hayden BY (2015) The psychology and neuroscience of curiosity. <i>Neuron</i> 88(3):449–460	1018
Kirilina E, Lutti A, Poser BA, et al (2016) The quest for the best: The impact of different epi sequences on the sensitivity of random effect fmri group analyses. <i>Neuroimage</i> 126:49–59	1019
Kringelbach ML, Rolls ET (2004) The functional neuroanatomy of the human orbitofrontal cortex: evidence from neuroimaging and neuropsychology. <i>Progress in neurobiology</i> 72(5):341–372	1020
Liu Q, Zhao Y, Attanti S, et al (2024) Midbrain signaling of identity prediction errors depends on orbitofrontal cortex networks. <i>Nature Communications</i> 15(1):1704	1021
Mackey S, Petrides M (2010) Quantitative demonstration of comparable architectonic areas within the ventromedial and lateral orbital frontal cortex in the human and the macaque monkey brains. <i>European Journal of Neuroscience</i> 32(11):1940–1950	1022
McDannald MA, Esber GR, Wegener MA, et al (2014) Orbitofrontal neurons acquire responses to ‘valueless’ pavlovian cues during unblocking. <i>Elife</i> 3:e02653	1023
McNamee D, Rangel A, O’doherty JP (2013) Category-dependent and category-independent goal-value codes in human ventromedial prefrontal cortex. <i>Nature neuroscience</i> 16(4):479–485	1024
Murray EA, O’Doherty JP, Schoenbaum G (2007) What we know and do not know about the functions of the orbitofrontal cortex after 20 years of cross-species studies. <i>Journal of Neuroscience</i> 27(31):8166–8169	1025
Murray EA, Moylan EJ, Saleem KS, et al (2015) Specialized areas for value updating and goal selection in the primate orbitofrontal cortex. <i>elife</i> 4:e11695	1026
	1027
	1028
	1029
	1030
	1031
	1032
	1033
	1034
	1035
	1036
	1037
	1038
	1039
	1040
	1041
	1042
	1043
	1044
	1045
	1046
	1047
	1048
	1049
	1050
	1051
	1052
	1053
	1054
	1055
	1056
	1057
	1058

- 1059 Myung JI, Karabatsos G, Iverson GJ (2005) A bayesian approach to testing decision  
1060 making axioms. *Journal of Mathematical Psychology* 49(3):205–225  
1061
- 1062 Namboodiri VMK, Otis JM, van Heeswijk K, et al (2019) Single-cell activity tracking  
1063 reveals that orbitofrontal neurons acquire and maintain a long-term memory to  
1064 guide behavioral adaptation. *Nature neuroscience* 22(7):1110–1121  
1065
- 1066 Neubert FX, Mars RB, Sallet J, et al (2015) Connectivity reveals relationship of brain  
1067 areas for reward-guided learning and decision making in human and monkey frontal  
1068 cortex. *Proceedings of the national academy of sciences* 112(20):E2695–E2704  
1069
- 1070 O'doherty J, Rolls ET, Francis S, et al (2000) Sensory-specific satiety-related olfactory  
1071 activation of the human orbitofrontal cortex. *Neuroreport* 11(4):893–897  
1072
- 1073 O'Doherty J, Kringelbach ML, Rolls ET, et al (2001) Abstract reward and punishment  
1074 representations in the human orbitofrontal cortex. *Nature neuroscience* 4(1):95–102  
1075
- 1076 O'keefe J, Nadel L (1978) The hippocampus as a cognitive map. Oxford university  
1077 press  
1078
- 1079 Ostlund SB, Balleine BW (2007) Orbitofrontal cortex mediates outcome encoding in  
1080 pavlovian but not instrumental conditioning. *Journal of Neuroscience* 27(18):4819–  
1081 4825  
1082
- 1083 Ouellet J, McGirr A, Van den Eynde F, et al (2015) Enhancing decision-making and  
1084 cognitive impulse control with transcranial direct current stimulation (tdcs) applied  
1085 over the orbitofrontal cortex (ofc): a randomized and sham-controlled exploratory  
1086 study. *Journal of psychiatric research* 69:27–34  
1087
- 1088 Panayi MC, Killcross S (2021) The role of the rodent lateral orbitofrontal cortex in  
1089 simple pavlovian cue-outcome learning depends on training experience. *Cerebral  
Cortex Communications* 2(1):tgab010  
1090
- 1091 Pickens CL, Saddoris MP, Setlow B, et al (2003) Different roles for orbitofrontal cortex  
1092 and basolateral amygdala in a reinforcer devaluation task. *Journal of Neuroscience*  
1093 23(35):11078–11084  
1094
- 1095 Poser BA, Versluis MJ, Hoogduin JM, et al (2006) Bold contrast sensitivity enhance-  
1096 ment and artifact reduction with multiecho epi: parallel-acquired inhomogeneity-  
1097 desensitized fmri. *Magnetic Resonance in Medicine: An Official Journal of the  
International Society for Magnetic Resonance in Medicine* 55(6):1227–1235  
1098
- 1099 Price JL (2007) Definition of the orbital cortex in relation to specific connections with  
1100 limbic and visceral structures and other cortical regions. *Annals of the New York  
1101 Academy of Sciences* 1121(1):54–71  
1102  
1103  
1104

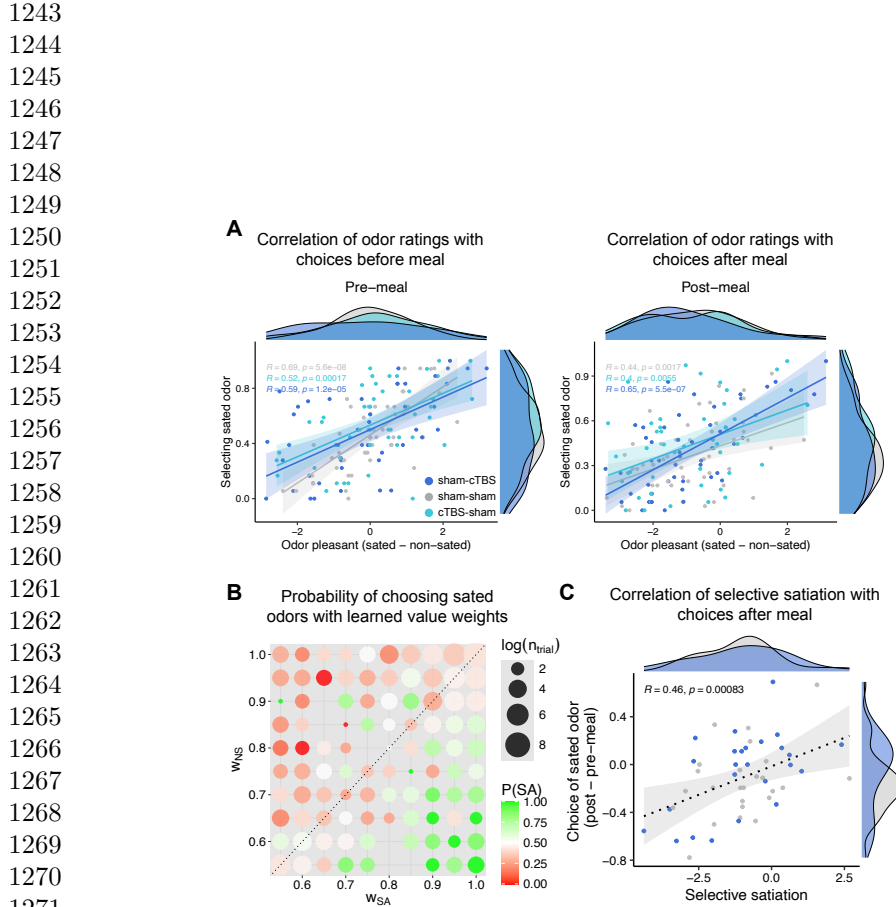
Rhodes SE, Murray EA (2013) Differential effects of amygdala, orbital prefrontal cortex, and prelimbic cortex lesions on goal-directed behavior in rhesus macaques. <i>Journal of Neuroscience</i> 33(8):3380–3389	1105 1106 1107 1108 1109 1110 1111 1112 1113 1114 1115 1116 1117 1118 1119
Rich EL, Wallis JD (2017) Spatiotemporal dynamics of information encoding revealed in orbitofrontal high-gamma. <i>Nature Communications</i> 8(1):1139	1108 1109 1110 1111 1112 1113
Rizley RC, Rescorla RA (1972) Associations in second-order conditioning and sensory preconditioning. <i>Journal of comparative and physiological psychology</i> 81(1):1	1111 1112 1113
Rudebeck PH, Murray EA (2014) The orbitofrontal oracle: cortical mechanisms for the prediction and evaluation of specific behavioral outcomes. <i>Neuron</i> 84(6):1143–1156	1114 1115 1116
Schuck NW, Cai MB, Wilson RC, et al (2016) Human orbitofrontal cortex represents a cognitive map of state space. <i>Neuron</i> 91(6):1402–1412	1117 1118 1119
Spiegelhalter DJ, Best NG, Carlin BP, et al (2002) Bayesian measures of model complexity and fit. <i>Journal of the royal statistical society: Series b (statistical methodology)</i> 64(4):583–639	1120 1121 1122 1123
Stalnaker TA, Cooch NK, McDannald MA, et al (2014) Orbitofrontal neurons infer the value and identity of predicted outcomes. <i>Nature communications</i> 5(1):3926	1124 1125 1126
Stoll FM, Rudebeck PH (2024) Dissociable representations of decision variables within subdivisions of the macaque orbital and ventrolateral frontal cortex. <i>Journal of Neuroscience</i> 44(35)	1127 1128 1129
Tegelbeckers J, Porter DB, Voss JL, et al (2023) Lateral orbitofrontal cortex integrates predictive information across multiple cues to guide behavior. <i>Current Biology</i> 33(20):4496–4504. e5	1130 1131 1132 1133
Tolman EC (1948) Cognitive maps in rats and men. <i>Psychological review</i> 55(4):189	1134 1135
Vaidya AR, Badre D (2022) Abstract task representations for inference and control. <i>Trends in cognitive sciences</i> 26(6):484–498	1136 1137 1138
Wallis JD (2012) Cross-species studies of orbitofrontal cortex and value-based decision-making. <i>Nature neuroscience</i> 15(1):13–19	1139 1140 1141
Walton ME, Behrens TE, Noonan MP, et al (2011) Giving credit where credit is due: orbitofrontal cortex and valuation in an uncertain world. <i>Annals of the New York Academy of Sciences</i> 1239(1):14–24	1142 1143 1144 1145
Wang F, Howard JD, Voss JL, et al (2020) Targeted stimulation of an orbitofrontal network disrupts decisions based on inferred, not experienced outcomes. <i>Journal of Neuroscience</i> 40(45):8726–8733	1146 1147 1148 1149 1150

- 1151 Wang MZ, Hayden BY (2021) Latent learning, cognitive maps, and curiosity. Current  
1152 Opinion in Behavioral Sciences 38:1–7  
1153  
1154 Wang MZ, Hayden BY, Heilbronner SR (2022) A structural and functional subdivision  
1155 in central orbitofrontal cortex. Nature communications 13(1):3623  
1156  
1157 Wilson RC, Takahashi YK, Schoenbaum G, et al (2014) Orbitofrontal cortex as a  
1158 cognitive map of task space. Neuron 81(2):267–279  
1159  
1160 Xia M, Wang J, He Y (2013) Brainnet viewer: a network visualization tool for human  
1161 brain connectomics. PloS one 8(7):e68910  
1162  
1163 Zhao LS, Raithel CU, Tisdall MD, et al (2024) Leveraging multi-echo epi to enhance  
1164 bold sensitivity in task-based olfactory fmri. Imaging Neuroscience 2:1–15  
1165  
1166 Zhou J, Montesinos-Cartagena M, Wikenheiser AM, et al (2019) Complementary task  
1167 structure representations in hippocampus and orbitofrontal cortex during an odor  
1168 sequence task. Current Biology 29(20):3402–3409. e3  
1169  
1170  
1171  
1172  
1173  
1174  
1175  
1176  
1177  
1178  
1179  
1180  
1181  
1182  
1183  
1184  
1185  
1186  
1187  
1188  
1189  
1190  
1191  
1192  
1193  
1194  
1195  
1196

1197  
 1198  
 1199  
 1200  
 1201  
 1202  
 1203  
 1204  
 1205  
 1206  
 1207  
 1208  
 1209  
 1210  
 1211  
 1212  
 1213  
 1214  
 1215  
 1216  
 1217  
 1218  
 1219  
 1220  
 1221  
 1222  
 1223  
 1224  
 1225  
 1226  
 1227  
 1228  
 1229  
 1230  
 1231  
 1232  
 1233  
 1234  
 1235  
 1236  
 1237  
 1238  
 1239  
 1240  
 1241  
 1242

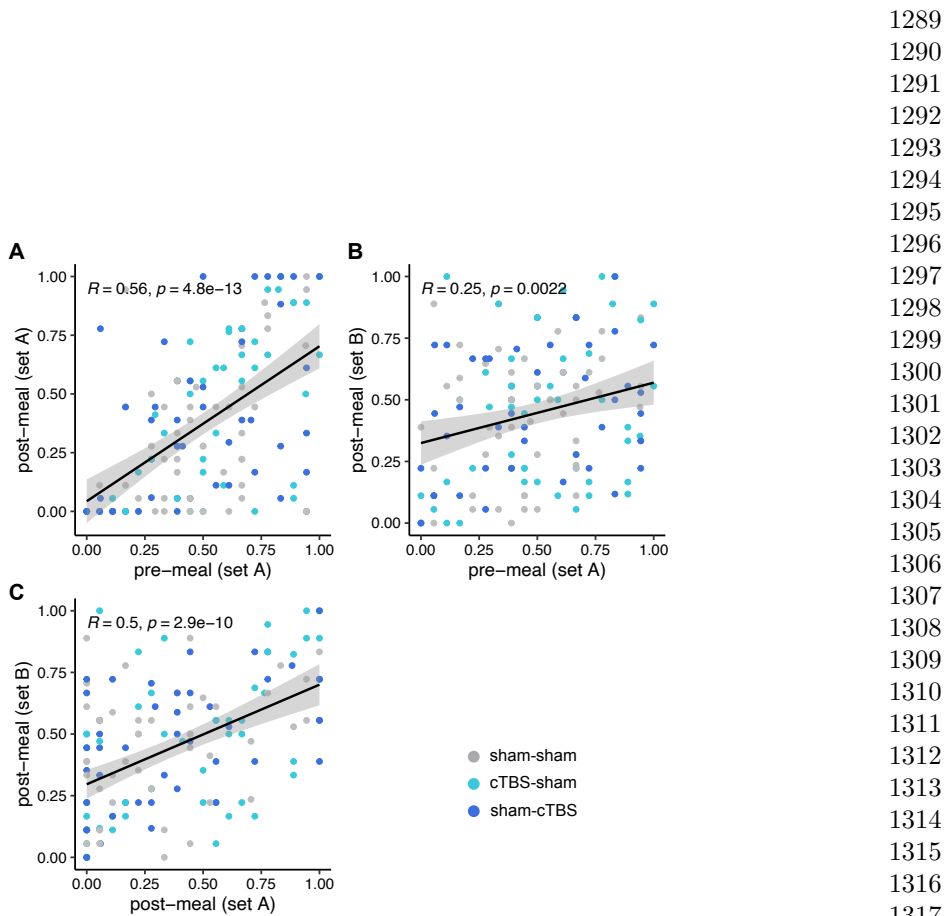


**Extended Data Fig. 1: Supplementary results on odor pleasantness ratings across stimulation conditions and sessions.** **A.** Odor pleasantness ratings separated by TMS condition (sham–sham, cTBS–sham, sham–cTBS), stimulation target (aOFC vs. pOFC), and odor type (sated vs. non-sated), displayed for pre- and post-meal timepoints. These ratings confirm that selective satiation effects were robust across TMS conditions within each target group. **B.** Odor pleasantness ratings by session number (1, 2, 3), stimulation target, and odor type, again separated into pre- and post-meal measurements. This panel examines potential habituation or learning effects across repeated exposures. No evidence of habituation was observed, and satiation effects remained consistent across sessions within each target group.



1273 **Extended Data Fig. 2: Probe choices are influenced by learned stimulus values and selective satiation effects.** **A.** Scatter plots showing correlations  
1274 between the choice of stimuli predicting sated odors and odor pleasantness ratings of  
1275 sated minus non-sated odors before (left) and after the meal (right), separated by the  
1276 three TMS conditions. **B.** Choice of sated odors options associated with each of the  
1277 learned weight of the combination of sated and non-sated options. Dot size represents  
1278 the number of trials per value combination (log-scaled), with missing dots indicating  
1279 unobserved combinations. **C.** Scatter plots showing correlations between selective  
1280 satiation effect and choices of sated odor.

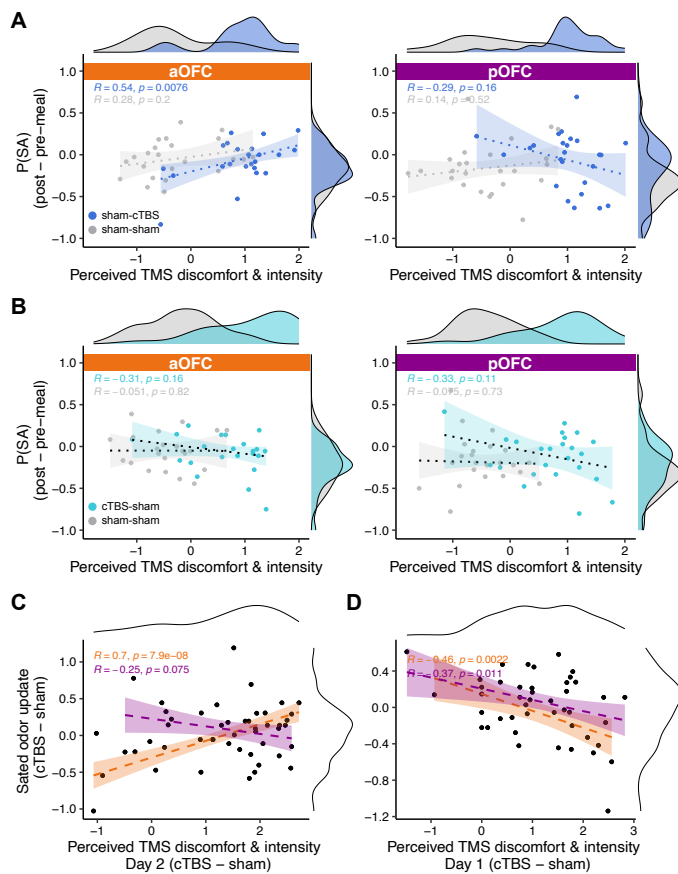
1281  
1282  
1283  
1284  
1285  
1286  
1287  
1288



**Extended Data Fig. 3: Scatter plots showing correlations in the proportion of sated odor choices across different sessions and odor sets. A.** Correlation between pre-meal and post-meal choices for odors in Set A. **B.** Correlation between pre-meal choices for Set A and post-meal choices for Set B. **C.** Correlation between post-meal choices for Set A and Set B. Each dot represents a participant. Reported Pearson's  $R$  and  $p$  values are calculated across all participants, collapsing across TMS conditions due to the absence of significant differences. These correlations reflect stable individual patterns in sated odor choice behavior across TMS conditions and stimulus sets.

1289  
1290  
1291  
1292  
1293  
1294  
1295  
1296  
1297  
1298  
1299  
1300  
1301  
1302  
1303  
1304  
1305  
1306  
1307  
1308  
1309  
1310  
1311  
1312  
1313  
1314  
1315  
1316  
1317  
1318  
1319  
1320  
1321  
1322  
1323  
1324  
1325  
1326  
1327  
1328  
1329  
1330  
1331  
1332  
1333  
1334

1335  
 1336  
 1337  
 1338  
 1339  
 1340  
 1341  
 1342  
 1343  
 1344  
 1345  
 1346  
 1347  
 1348  
 1349  
 1350  
 1351  
 1352  
 1353  
 1354  
 1355  
 1356  
 1357  
 1358  
 1359  
 1360  
 1361  
 1362  
 1363  
 1364  
 1365  
 1366  
 1367  
 1368  
 1369  
 1370  
 1371  
 1372  
 1373  
 1374  
 1375  
 1376  
 1377  
 1378  
 1379  
 1380



**Extended Data Fig. 4: Relationship between perceived TMS discomfort and intensity and sated odor (SA) choices.** **A.** Correlation between SA choices and TMS ratings, separated by Day 2 TMS conditions (sham-cTBS vs. sham-sham) and TMS targeted regions (aOFC, pOFC). A positive correlation was observed between TMS ratings and SA choices in the aOFC group, but including ratings of TMS perception into the regression models did not alter the observed TMS effects on SA choices. **B.** Same as **A**, but focus on Day 1 TMS effect (sham-sham vs. cTBS-sham). **C.** Scatter plot showing the relationship between the condition-wise difference (sham-cTBS vs. sham-sham) of SA choices and condition-wise difference of TMS ratings from Day 2 TMS. There was a significant positive correlation in the aOFC group (Pearson's  $r = 0.7, p = 7.9e-8$ ) **D.** Same as **B**, but focus on Day 1 TMS effect (sham-sham vs. cTBS-sham). Shaded areas represent 95% confidence intervals estimated using robust linear regression. Marginal distributions are shown on the top and right axes. Pearson correlation coefficients ( $R$ ) and p-values are reported for each TMS condition.